Published in final edited form as:
Atmos Environ (1994). 2017 ; 154: 42–52. doi:10.1016/j.atmosenv.2017.01.040.

Does temperature nudging overwhelm aerosol radiative effects in regional integrated climate models?

Jian He[a,*], **Timothy Glotfelty**[a], **Khairunnisa Yahya**[b], **Kiran Alapaty**[a], and **Shaocai Yu**[c,d,**]

[a]Systems Exposure Division, National Exposure Research Laboratory, U.S. Environmental Protection Agency, Research Triangle Park, NC 27711, USA

[b]Department of Marine, Earth, and Atmospheric Sciences, North Carolina State University, Raleigh, NC 27695, USA

[c]Research Center for Air Pollution and Health, Ministry of Education, College of Environmental and Resource Sciences, Zhejiang University, Hangzhou, Zhejiang 310058, PR China

[d]Key Laboratory of Environmental Remediation and Ecological Health, Ministry of Education, College of Environmental and Resource Sciences, Zhejiang University, Hangzhou, Zhejiang 310058, PR China

Abstract

Nudging (data assimilation) is used in many regional integrated meteorology-air quality models to reduce biases in simulated climatology. However, in such modeling systems, temperature changes due to nudging could compete with temperature changes induced by radiatively active and hygroscopic short-lived tracers leading to two interesting dilemmas: when nudging is continuously applied, what are the relative sizes of these two radiative forces at regional and local scales? How do these two forces present in the free atmosphere differ from those present at the surface? This work studies these two issues by converting temperature changes due to nudging into pseudo radiative effects (PRE) at the surface (PRE_sfc), in troposphere (PRE_atm), and at the top of atmosphere (PRE_toa), and comparing PRE with the reported aerosol radiative effects (ARE). Results show that the domain-averaged PRE_sfc is smaller than ARE_sfc estimated in previous studies and this work, but could be significantly larger than ARE_sfc at local scales. PRE_atm is also much smaller than ARE_atm. These results indicate that appropriate nudging methodology could be applied to the integrated models to study aerosol radiative effects at continental/regional scales, but it should be treated with caution for local scale applications.

Keywords

Nudging; Aerosol radiative effects; Integrated models; Regional climate

*Corresponding author. jianhe.phd@gmail.com (J. He). **Corresponding author. Research Center for Air Pollution and Health, Ministry of Education, College of Environmental and Resource Sciences, Zhejiang University, Hangzhou, Zhejiang 310058, PR China. shaocaiyu@zju.edu.cn (S. Yu).

Appendix A. Supplementary data
Supplementary data related to this article can be found at http://dx.doi.org/10.1016/j.atmosenv.2017.01.040.

1. Introduction

Meteorology is an important driver for chemical transport models, popularly known as air quality models. Several studies have documented the importance and impacts of meteorology (e.g., temperature, wind, and humidity) on air quality predictions (Jacob and Winner, 2009; Godowitch et al., 2011). Thus, to generate better meteorological inputs, nudging methodologies have been used to drive off-line air quality models to improve model's capability to simulate and understand chemistry/aerosols at global scales (Jöckel et al., 2006; Tilmes et al., 2015; He et al., 2015) and regional scales (e.g., Binkowski and Roselle, 2003). With the rapid development of computer resources and improved understanding of meteorology-chemistry interactions, several integrated or on-line coupled models (which include impacts of air pollutants on meteorology) have been developed to study feedbacks associated with the climate-chemistry-aerosol-cloud-radiation system (e.g., Zhang, 2008). For example, the Weather Research and Forecasting model integrated with a Chemistry model (WRF-Chem, Grell et al., 2005; Fast et al., 2006) and the two-way coupled WRF with the Community Multiscale Air Quality Modeling System (WRF-CMAQ, Wong et al., 2012) were developed to estimate the direct and indirect effects of aerosol on regional scales (Forkel et al., 2012; Yu et al., 2014; Wang et al., 2015).

Due to the complex nature of these coupled models, it is more challenging to accurately simulate meteorology. Currently, there are two commonly utilized approaches applied to the integrated models for a precise simulation of meteorology. One approach is to apply frequent re-initialization to the meteorological variables (e.g., temperature, specific humidity, and wind speed), which is widely used in the Air Quality Model Evaluation International Initiative (AQMEII) project. For example, Forkel et al. (2015) used the WRF-Chem model with a 2-day cyclic re-initialization of meteorological fields, which resulted in seasonal mean solar radiation and temperature decreasing by 20 W m^{-2} and 0.25 °C, respectively, due to the aerosol direct effects during the 2010 Russian summer wildfire episode. Applying the same model, Wang et al. (2015) found that the overall aerosol effects on the net surface solar radiation and 2-m temperature would be −16.2 W m^{-2} and −0.05 °C, respectively, over North America for July 2006. Although this approach can improve meteorology, abrupt changes at the end of each re-initialization period and consequent model spin-up result in discontinuity in the simulation of meteorological fields. Additionally, frequent re-initialization could dampen the feedback from the aerosol-radiation system. Alternatively, another common approach is to use nudging to produce better meteorology for air quality simulations (e.g., Vautard et al., 2012; Hogrefe et al., 2015), which is also used in many integrated models to study the aerosol-radiation interactions. For example, by using the WRF-Chem model with analysis nudging, Kumar et al. (2014) found that the radiative perturbation due to dust aerosols is about −2.9 ± 3.1 W m^{-2} at the top of the atmosphere, 5.1 ± 3.3 W m^{-2} in the atmosphere, and −8.0 ± 3.3 W m^{-2} at the surface, based on the sub-region averages in northern India. Using the WRF-CMAQ model with analysis nudging, Hogrefe et al. (2015) found that decreases of $PM_{2.5}$ between 2006 and 2010 resulted in simulated increases of summer mean clear-sky shortwave radiation between 5 and 10 W m^{-2}. One limitation of this approach is that nudging could dampen the feedback from the aerosol-radiation system. Although most studies acknowledge this limitation, many do not

quantify the impacts from nudging and aerosols separately. In a one-month simulation of a sensitivity test (e.g., with/without nudging or aerosol direct feedback) with frequent model re-initialization, Hogrefe et al. (2015) determined that a weak nudging can slightly improve the representation of domain averages of 2-m air temperatures for retrospective air quality applications without overwhelming the simulated feedback effects. This result is expected because of frequent re-initialization used in the simulations. However, it is not clear how their selection of weak nudging impacted free atmospheric prognostic fields (e.g., temperature, mixing ratio, and cloud fields) and what would be the outcome if their model was run in a continuous mode without any re-initialization. But, they stated that additional tests are needed to quantify these two competing forces (nudging vs aerosol direct effects). When an integrated or coupled model is continuously run without any re-initialization and nudging, 2-m temperatures, as well as free atmospheric parameters, can be affected largely at local scales, although this aspect has also not been studied or documented in the literature. Weak coefficients used for tropospheric nudging by Hogrefe et al. (2015) are the same as those suggested by Bullock et al. (2014). However, Bullock et al. (2014) documented advantages and disadvantages of using such weak coefficients in their large spatial and time scale study. They found that stronger nudging coefficients minimizes modeling errors, but strong nudging might dominate over model forcing by various physical processes. However, weaker nudging coefficients led to mixed results - errors in temperature fields were still contained while moisture errors were not. One likely issue with using weak nudging coefficients is that for pristine and less polluted regions and/or periods when cloud processes remove pollution, reduced or weaker nudging coefficients can lead to increased integrated or coupled model errors.

Due to the uncertainties inherent in the regional climate modeling systems, model simulations (e.g., temperature) may drift from observed climate without using a nudging methodology. For example, several decadal regional climate simulation studies reported that without interior nudging, biases in monthly 2-m temperature can be greater than 4 K over the continental U.S. (e.g., Otte et al., 2012). These studies also reported that seasonal surface precipitation is more accurately simulated when a nudging methodology is applied (Bowden et al., 2013). Several studies have also demonstrated that nudging is required to develop credible climate simulations (Jöckel et al., 2006; Zhang et al., 2014). To further improve retrospective modeling simulations, indirect soil moisture nudging methods (e.g., Mahfouf, 1991; Hogrefe et al., 2015) as well as direct nudging methods for improving surface air temperature and moisture coupled with indirect nudging of soil temperature and moisture (e.g., Alapaty et al., 2008, 2016) have been developed in recent years.

Nudging of atmospheric temperature, though artificial, could compete with that of temperature changes induced by radiatively active and hygroscopic short-lived tracers. Since the associated radiative impacts due to nudging were included in many integrated (online coupled) meteorology-air quality models (here after referred to as integrated models), it poses two intriguing dilemmas: when nudging is continuously applied, what are the relative sizes of these two radiative forces (i.e., temperature changes due to nudging vs. temperature changes due to aerosol effects) at regional and local scales? How do these two forces present in the free atmosphere differ from those present at the surface? This work addressed these important questions by converting model simulated temperature tendencies due to nudging

into radiative effects, referred to as pseudo radiative effects (PRE), through performing seasonal regional climate simulations for the central and eastern U.S. using the Weather Research & Forecasting (WRF) model. Reasons for not using an integrated model in this study are two-fold: (1) to clearly demonstrate whether or not a coupled model is truly needed for regional climate simulations; and (2) aerosol radiative effects were already quantified by using several measurements, as well as global and regional coupled models. Therefore, in this work, reported sizes of aerosol radiative effects were collected and compared with PRE due to nudging obtained from using the WRF model. Our rationale is further discussed in the next section.

2. Methodology

In this work, tropospheric nudging and surface nudging are used in the continuous WRF model simulations. The Four-Dimensional Data Assimilation (FDDA, Stauffer and Seaman, 1990, 1994) method has been widely used for tropospheric nudging. This method was demonstrated to reduce simulated meteorological biases, and has been applied for many air quality studies (Godowitch et al., 2011; Gilliam et al., 2012). To reduce surface biases in meteorological predictions, flux-adjusting surface data assimilation system (FASDAS) was developed by Alapaty et al. (2008, 2016) to provide continuous adjustments for three dimensional soil moisture, soil skin temperature, surface air temperature and water vapor mixing ratio. Unlike many other surface nudging approaches (either direct methods or indirect methods), FASDAS is comprised of both the direct nudging of atmospheric surface layer as well as the indirect nudging of soil temperature and soil moisture. Thus, the FASDAS corrects and adjusts both the land surface and atmospheric variables to maintain thermodynamic consistency (Alapaty et al., 2008). For direct nudging, FASDAS corrects errors inherent in all physical and dynamical processes affecting surface temperatures/moistures. The indirect nudging method converts this information into respective adjustment heat fluxes to adjust soil heat fluxes in order to account for uncertainties in soil temperature and moisture-related processes including initial conditions. Note that the magnitudes of coefficients used in other surface nudging methods are solely based on heuristic arguments and/or trial-error approaches. Many studies using such methods tend to tune these coefficients to the specific needs of the study. On the other hand, the magnitude of nudging coefficients used in FASDAS are fixed and are based on a physical methodology, which is related to the time scale of the largest turbulent eddies of convective boundary layer (Alapaty et al., 2008).

Based on the FASDAS and FDDA nudging methods, the equations below are used to calculate the pseudo radiative effects at surface (PRE_sfc), within the troposphere (PRE_atm), and at the top of the atmosphere (PRE_toa). PRE_sfc is estimated as the combination of the surface adjustment sensible heat flux and surface adjustment latent heat flux (Eqs. (1)–(3)) obtained from the FASDAS method. For troposphere, temperature tendencies due to nudging are converted into radiative heat flux (Eq. (4)) using the FDDA method. To facilitate a simple comparison, tropospheric effects are calculated by vertically averaging the PRE for all model layers above boundary layer, and refer to it as PRE_atm. Thus, PRE is estimated as:

$$H_S^F = \rho C_p \left(\frac{\partial T_a^F}{\partial t} \right) \Delta Z \quad (1)$$

$$H_l^F = \rho L \left(\frac{\partial q_a^F}{\partial t} \right) \Delta Z \quad (2)$$

$$PRE\_sfc = \left\{ H_S^F - \psi_q H_l^F \right\}_{sfc} \quad (3)$$

where H_S^F and H_l^F are, respectively, the surface adjustment sensible and latent heat flux (W m^{-2}) due to nudging; ρ is air density (kg m^{-3}); C_p is specific heat for air at constant pressure (J kg^{-1} K^{-1}); L is the latent heat due to condensation (J kg^{-1}); $\frac{\partial T_a^F}{\partial t}$ and $\frac{\partial q_a^F}{\partial t}$ are, respectively, the rate of change of the air temperature (K s^{-1}) and water vapor mixing ratio (kg kg^{-1} s^{-1}) due to nudging; Δz is the thickness of atmospheric layer (m); and ψ_q is the normalized weighting factor for soil moisture adjustment. Now, free tropospheric pseudo radiative effect due to nudging can be estimated as:

$$PRE\_atm = \frac{1}{n} \sum_{pbl}^{top} H_S^F \quad (4)$$

where n is the total number of model layers between planetary boundary layer (*pbl*) top and model top. Note no nudging is applied within boundary layer. The net or the top of the atmosphere pseudo radiative effect, PRE_toa, can be estimated as the sum of PRE_sfc and PRE_atm as follows:

$$PRE\_toa = PRE\_sfc + PRE\_atm \quad (5)$$

Instead of conducting two separate simulations to derive these effects, additional code was added to the model to calculate PRE_sfc and PRE_atm at each time step for each grid cell within one simulation. PRE_sfc and PRE_atm are in the model output on an hourly basis. In this case, the values of PRE_sfc, PRE_atm, and PRE_toa directly represent the instantaneous impacts from nudging. PRE_sfc, PRE_atm, and PRE_toa can either be positive (i.e., nudging has a warming effect), indicating the model underpredicts temperatures, or negative (i.e., nudging has a cooling effect), indicating the model overpredicts temperatures.

Table 1 summarizes WRF simulations conducted in this work. The WRF (version 3.7.1) model simulations are performed covering central and eastern U.S. for June, July, and August (JJA) 2006 with 12-km horizontal grid resolution and 35 vertical layers from surface to 50 hPa. Instead of applying frequent re-initializations, continuous simulations are conducted by applying FDDA for free tropo-sphere and FASDAS for surface (referred to as CNTL). A sensitivity study with FDDA for the free troposphere only (referred to as EXPA) is also conducted and compared to CNTL to show the impacts of FASDAS on surface predictions. In both CNTL and EXPA, no aerosols are included in the radiation calculation (i.e., aer_opt = 0 in the namelist). However, the magnitudes of PRE would change if aerosols are included in the radiation calculation. Due to the computational expediency, a WRF simulation with chemistry is not conducted in this work. Instead, to get the instantaneous impacts of aerosol radiative effects, double calls were added to the radiation scheme in a third WRF simulation (referred to as EXPB) to calculate differences in shortwave fluxes between prescribed aerosol condition (i.e., aer_opt = 1) and no aerosol condition (i.e., aer_opt = 0). Since this is a WRF only simulation without fully prognostic aerosol-cloud interactions, aerosol radiative effects (ARE) estimated in EXPB are only for direct radiative effects, and are defined as the changes in net shortwave radiative fluxes due to prescribed aerosol optical properties. ARE is calculated at the top of atmosphere (ARE_toa), in atmosphere (ARE_atm) and at the surface (ARE_sfc), respectively.

Major physics options used in the model configuration include the shortwave and longwave radiation scheme based on the Rapid Radiative Transfer Method for general circulation models (RRTMG, Mlawer et al., 1997; Iacono et al., 2008), surface layer scheme based on Monin-Obukhov Similarity theory (Monin and Obukhov, 1954), planetary boundary layer scheme of Yonsei University (Hong et al., 2006), the National Centers for Environmental Prediction, Oregon State University, Air Force, and Hydrologic Research Lab-NWS Land Surface Model (NOAH LSM) (Chen and Dudhia, 2001; Ek et al., 2003), microphysics scheme of Morrison et al. (2009), and cumulus scheme based on the Multi-Scale Kain-Fritsch (MSKF) scheme of Alapaty et al. (2014) and Zheng et al. (2016). FASDAS is applied for surface nudging with relaxation coefficients of 8.3×10^{-4} s^{-1} for both temperature and moisture. The nudging coefficients for surface are based on the turnover time scale (i.e., 20 min) of the largest turbulent eddies of the convection boundary layer (Alapaty et al., 2008). Weak analysis nudging is applied for the free atmosphere with relaxation coefficients of 5.0×10^{-5} s^{-1} for temperature and horizontal wind (i.e., u-v components), and 5.0×10^{-6} s^{-1} for moisture to allow maximum internal and numerical consistency in simulating meteorological processes. These nudging coefficients for free atmosphere are selected through sensitivity tests in Bullock et al. (2014) for their model configurations despite documented pros and cons of using such weak nudging coefficients. No nudging is applied within the PBL. Initial and lateral boundary conditions are obtained from the National Center for Environmental Prediction (NCEP) North American Model (NAM) output through the WRF Pre-processing System (WPS). Observations for upper air and surface nudging are obtained from the Meteorological Assimilation Data Ingest System (MADIS) and the National Center for Atmospheric Research (NCAR), respectively. The surface nudging files are generated by the OBSGRID utility provided by NCAR.

3. Results and discussion

3.1. Impacts of FASDAS on surface predictions

Surface air is nudged using surface reanalyses products at each time step and each grid cell utilizing the FASDAS. Fig. 1 shows 2-m temperature (T2) and 2-m water vapor mixing ratio (Q2) deviations from three model simulations (i.e., model – observations). Independent surface measurement data, known as Quality Controlled Local Climatological Data (http://www.ncdc.noaa.gov/orders/qclcd/), are used to generate results shown in Fig. 1. As shown in Fig. 1a, T2 bias increases (e.g., from 0.5 °C to 3 °C) as the EXPA simulation continues. With the FASDAS applied to the WRF (i.e., CNTL), T2 bias is smaller than that in EXPA by up to 1 °C. This shows a significant impact of FASDAS on surface temperature predictions. Similarly, Q2 bias in CNTL is smaller than that in EXPA by up to 3 g kg^{-1} (See Fig. 1b). However, there is not much difference in T2 and Q2 biases between CNTL and EXPB, except that there is a slightly larger cool bias in nighttime T2 and slightly smaller warm bias in daytime T2 by EXPB. The mean bias of T2 and Q2 against QCLCD are shown in Figure S1 in the supplementary material. In general, the performance of EXPB is very similar to CNTL, with slightly lower root mean square error (RMSE) and better correlation coefficient (R).

Fig. 2 shows the impacts of FASDAS on precipitation predictions. Precipitation data from Parameter elevation Regression on Independent Slopes Model (PRISM, Daly et al., 1994) is used to evaluate the predicted precipitation by WRF simulations. As shown in Fig. 2, FASDAS is able to reduce the dry bias of accumulated precipitation over middle and eastern domain despite underestimating precipitation intensity. In addition, FASDAS is able to reduce the wet bias of accumulated precipitation over eastern coastal regions as well. Compared to PRISM data, CNTL is better than EXPA in terms of spatial distribution and intensity of precipitation, since FASDAS can correct the temperature and moisture biases in CNTL. Precipitation predicted by EXPB is very similar to that by CNTL in terms of spatial distribution and intensity (figure not shown). The impacts from EXPB on precipitation are very small because only prescribed aerosol optical properties are used for radiation calculations and cloud droplet number concentrations are held constant in the Morrison scheme.

3.2. Estimated PRE and ARE

Surface temperature differences between with and without nudging simulations are converted to PRE_sfc (Eqs. (1)–(3)) for comparison with ARE_sfc. Similarly, following Eq. (4), PRE_atm and PRE_toa are obtained using Eq. (5). Fig. 3 shows spatial distribution of JJA averages of PRE_sfc, PRE_atm, and PRE_toa from CNTL and EXPB, as well as ARE_sfc, ARE_atm, and ARE_toa under clear-sky conditions. Interestingly, in CNTL, PRE_sfc is negative over most of the domain except over mountains and domain boundaries where surface observations may be sparse or lacking. The positive PRE_sfc over mountains indicate model underpredicts surface temperatures over mountains. Similar model biases also occur over Tibet Plateau as presented in Ji and Kang (2013, 2015). The subgrid topography parameterization scheme in WRF can slightly affect PRE predictions (see Figure S2 in the supplementary material). However, these changes are not significant, especially

over the Appalachian Mountains, where PRE_sfc is positive. The negative PRE_sfc means nudging is cooling the surface, indicating the model overpredicts surface temperatures (also shown in Fig. 1). PRE_sfc vary over different observational sites, with a maximum cooling of −69.9 W m^{-2} (e.g., central domain) and a domain averaged cooling of −6.2 W m^{-2}. Similarly, PRE_atm is also negative over most of the domain, with small positive values along the boundaries. PRE_atm is calculated based on sparse sounding data (as compared to surface measurements). The circular patterns are caused by the modeling constraints such as the radius of influence of nudging to limit the influence of nudging for model grids far away from locations of observations. In general, the cooling effects are much smaller in the troposphere than at the surface, with a domain averaged cooling of −0.8 W m^{-2} in the troposphere. Therefore, PRE_toa (i.e., the sum of PRE_sfc and PRE_atm) is dominated by PRE_sfc, with a domain averaged cooling of −7.1 W m^{-2}.

With aerosol included in the radiation calculation in EXPB, the spatial distributions of PRE in EXPB are very similar to CNTL, but with smaller magnitudes in EXPB since ARE reduces the model's warm bias at the surface. The differences in absolute PRE between EXPB and CNTL are shown in Figure S3 in the supplementary material. As shown in Figure S3, PRE_sfc and PRE_toa in EXPB are generally lower than those in CNTL by up to 8.42 and 8.36 W m^{-2}, respectively. This indicates significant impacts from aerosols especially over the central U.S. and northeastern coast (>3 W m^{-2}) (although the domain averaged difference is relative small).

In EXPB, PRE_sfc varies from −68.7 to +22.1 W m^{-2}, with a domain average of −5.2 W m^{-2}. There is not much difference in PRE_atm between CNTL and EXPB, mainly due to the very limited observations for tropospheric nudging as well as weak nudging coefficient used in FDDA. As a result, PRE_toa in EXPB varies from −73.5 to +22.6 W m^{-2}, with a domain average of −6.1 W m^{-2}. For aerosol direct radiative effects, aerosols can affect shortwave radiation through absorption and scattering. As shown in Fig. 3, the aerosol scattering dominates at the surface, resulting in a domain averaged ARE_sfc of −8.7 W m^{-2}, whereas aerosol absorption dominates in troposphere, resulting in a domain averaged ARE_atm of +5.4 W m^{-2}, leading to ARE_toa with a domain average of −3.3 W m^{-2}. As shown in Fig. 3, the magnitudes of domain averages of ARE at surface and in troposphere are in general much larger than PRE, indicating ARE is significant at surface and in troposphere, even when nudging is applied. But due to combined cooling effects at the surface and warming effects in troposphere, ARE_toa is smaller than PRE_toa. It is important to note that the aerosol indirect radiative effects are not assessed in this study since cloud droplet number concentrations are held constant in the Morrison scheme and only prescribed aerosol optical properties are used for radiation calculation. These results indicate that at the surface FASDAS is correcting for errors introduced from the lack of ARE, but in the free troposphere FDDA nudging is compensating a portion of ARE due to errors in other model processes.

Seasonal (JJA) averaged PRE and ARE components are more significant at local sites than the domain averages. Fig. 4 shows the JJA averaged PRE and ARE components over New York City (NYC, 40.71° N, 74.00° W, urban site), the Ohio River Valley (ORV, 36.99° N, 89.13° W, rural site), the Southern Great Plains (SGP, 36.61° N, 97.49° W, semi-pristine

site), and the entire domain (DOM), respectively. Compared to domain averages, the cooling effects from nudging are much larger at the NYC and SGP sites. In CNTL, PRE is more significant at the SGP site (−22.2 W m^{-2} at surface, −2.4 W m^{-2} in atmosphere, and −24.6 W m^{-2} at top of atmosphere) than at the NYC site (−10.0 W m^{-2} at surface,−2.0 W m^{-2} in atmosphere, and −12.0 W m^{-2} at top of atmosphere) and the ORV site (−6.1 W m^{-2} at surface, +0.7 W m^{-2} in atmosphere, and −5.4 W m^{-2} at top of atmosphere). Differences in PRE_sfc among the SGP, NYC, and ORV sites are likely in part due to the differences (model vs actual) in anthropogenic land use, which can result in different land surface albedo, and therefore different radiative effects. Use of more accurate land use data could potentially reduce the model uncertainty. In addition, the land surface characteristics at SGP and NYC are quite different. SGP is a semi-pristine plain grass prairie environment site and NYC is an urban site. The surface soil moisture characteristics are different, and the nudging effects at these two sites are different. Also, there is no urban module turned on in WRF to simulate sophisticated urban processes, which is likely to result in large errors in surface predictions. A small positive PRE_atm at the ORV site indicates that nudging is warming the atmosphere (i.e., the model underpredicts temperatures in troposphere). However, PRE_sfc dominates the entire system and determines the warming or cooling trend of the modeled system. These results highlight the importance of a better representation of surface processes for high resolution regional climate simulations. Notably, urban climate simulations and future climate projections will be plagued by large surface errors if urban surface representations and related processes are not improved, posing a challenge to the integrated models.

Similar patterns of PRE are also shown in EXPB. Compared to PRE in EXPB, ARE varies from site to site. For example, ARE_sfc under all-sky (clear-sky) conditions is much smaller than PRE_sfc at the SGP site (i.e.,−9.8 (−10.9) W m^{-2} vs −19.8 W m^{-2}), whereas ARE_sfc is close to PRE_sfc at the NYC site under all-sky conditions(i.e., −7.7 W m^{-2} vs −7.9 W m^{-2}) and ARE_sfc is relatively larger than PRE_sfc at the ORV site (i.e., −9.1 (−10.3) W m^{-2} vs −4.2 W m^{-2}) under all-sky (clear-sky) conditions. Since EXPB used prescribed aerosol optical properties for shortwave radiation calculation, uncertainties exist in the ARE estimations. However, these results still demonstrate that nudging can possibly compete with or overwhelm aerosol effects at local scales.

Table 2 summarizes the reported aerosol radiative effects from previous studies. For example, Bellouin et al. (2013) estimated a JJA-mean shortwave direct radiative effect (DRE) from total aerosols at the top of the atmosphere with cooling effects by up to 10 W m^{-2} over North America under clear-sky conditions. Yu et al. (2006) also estimated a JJA-mean DRE on solar radiation at the top of the atmosphere, with values of −4.0 to −8.7 W m^{-2} from satellite estimations over North America under clear-sky conditions. Additionally, derived from measurements, Yu et al. (2006) reported a DRE with values of −5.2 to −11.1 W m^{-2} at the top of the atmosphere and −14.4 to −23.9 W m^{-2} at the surface. However, DRE in these studies are only for shortwave radiation, which can only represent the upper limit of DRE on total radiative fluxes (Yu et al., 2006); therefore, this may result in the overestimation of cooling effects by ~5–10% (Heald et al., 2014). Heald et al. (2014) estimated TOA DRE on total radiation fluxes with an annual mean of about −4 W m^{-2} for clear-sky conditions and about −2 W m^{-2} for all-sly conditions in mid-latitudes, whereas

summer mean DRE could be higher due to higher organic aerosols, especially over the eastern U.S. Alternatively, there are large uncertainties in the estimation of aerosol indirect effects. For example, Lohmann and Feichter (2005) found that the top-of-atmosphere radiative budget perturbation due to aerosol indirect effects vary from −0.5–5 W m^{-2} on global averages over land. Wang et al. (2015) showed that aerosol indirect effects lead to the reduction in the net surface solar radiation with a domain-wide mean of −12.1 W m^{-2} over continental U.S. during July 2006. Under all-sky conditions, the estimated ARE_sfc in this work is about −7.4 W m^{-2}, which is higher than −41 W m^{-2} estimated by Wang et al. (2015), mainly due to the different aerosol optical properties used in the calculation. ARE_atm estimated in this work is about +5.5 W m^{-2} on domain averages, which is comparable to that estimated by Matus (2013). ARE_toa is about −1.9 W m^{-2}, which is slightly lower than estimated by Matus (2013). Assuming aerosol indirect effects are of comparable magnitudes to aerosol direct effects over the U.S. as indicated by Leibensperger et al. (2012), domain-averaged PRE_toa in this work (i.e.,−7.1 W m^{-2}) is close to the lower limit of values estimated in Bellouin et al. (2013) and Yu et al. (2006), and also comparable to Heald et al. (2014). But PRE_sfc (i.e., −6.1 W m^{-2}) is lower than these reported values (even without considering aerosol indirect radiative effects). Therefore, using the integrated modeling system might reduce the model radiative bias for domain averages at the top of the atmosphere to some extent, but the inherent uncertainties in model surface processes still remain.

Fig. 5 shows the seasonal (JJA) averaged diurnal variation of PRE and ARE over NYC, ORV, SGP, and DOM. Trends in diurnal variations are somewhat similar but magnitudes of cooling/warming effects are different at each site. For example, the surface cooling effects (i.e., PRE_sfc) at the ORV site are smaller than at the SGP and NYC sites, suggesting the model predicts better surface temperatures at the ORV site. The PRE_sfc at the NYC site are negative in the afternoon, with a maximum cooling of −36.3 W m^{-2} at 1 300 EDT. This indicates the model overpredicts surface afternoon temperatures at the NYC site. Although higher concentrations of air pollutants can be expected in NYC than at the ORV and SGP sites, radiative effects induced by pollutants may not be able to reduce cold or warm biases in model simulations as compared to such large biases (i.e., PRE ~35 W m^{-2}) in an integrated modeling system. As shown in Fig. 5, ARE_sfc at NYC varies up to ~ −20 W m^{-2}, much smaller than PRE_sfc (up to −36 W m^{-2}) during the daytime. In this study, the NOAH LSM urban canopy model is not activated because to the best of our knowledge that urban canopy model was not validated for high resolution regional climate modeling for the US. However, an opportunity exists to later revisit this issue.

Unlike the ORV and NYC sites which have small positive PRE_sfc for certain times, the PRE_sfc at the SGP site is negative during the entire 24 h, indicating the model overpredicts surface temperatures at the SGP site all day long. For domain-averaged PRE_sfc (DOM), cooling effect is much smaller than that at other local site, with a maximum cooling of −9.2 W m^{-2}. At the ORV site, the PRE_atm is positive for most of time except during 1 500–1900 EDT, with a maximum warming of +2.0 W m^{-2} at 1 200 EDT. Unlike PRE_atm at the ORV site, PRE_atm at the NYC and SGP sites are negative during daytime, with maximum cooling of −4.7 and −4.2 W m^{-2}, respectively. For domain-averaged PRE_atm, the magnitude is relatively small, with a maximum cooling of −1.9 W m^{-2}. However, ARE_atm

is positive during the daytime, mainly due to the aerosol absorption. PRE_toa is dominated by PRE_sfc, with 24-h averages of −0.9, −12.0, −21.8, and −4.9 W m^{-2} at ORV, NYC, SGP, and DOM, respectively, whereas the 24-h averages of ARE_toa are −3.3, −3.8, −3.4 and −3.1 W m^{-2} at ORV, NYC, SGP, and DOM, respectively. Unlike PRE_toa, ARE_toa is combination of atmospheric heating and surface scattering. On the domain averages, ARE_toa is close to PRE_toa. But at local sites (e.g., NYC and SGP), the magnitudes of ARE_toa are much smaller than that of PRE_toa. Kassianov et al. (2013) found that strong diurnal changes of aerosol concentrations (e.g., 20%) have little impact on the 24-h average aerosol direct radiative effects at the top of atmosphere. But one would expect large changes in diurnal variation of radiative effects at the top of atmosphere with substantial changes in aerosol loadings (e.g., ≥80%), also indicated in Kassianov et al. (2013). As shown in Kassianov et al. (2013), aerosol direct radiative effects at a specific site vary under different aerosol concentration conditions, with a maximum cooling of about −8.5 W m^{-2} for low aerosol loading (on July 22, 2012) and about −40 W m^{-2} for ~ 80% higher aerosol loading (on August 30, 2012). Therefore, a substantial increase (~80%) in aerosol concentrations can increase ARE_toa by about 30 W m^{-2}. However, the PRE_toa at polluted sites (e.g., NYC) can be as large as −100 W m^{-2} in a single day (Figure not shown). Hence, in this case, PRE could overwhelm aerosol radiative effects at some polluted sites.

For the model configurations used in this study, the WRF model continues to overpredict surface temperatures without nudging as documented by Otte et al. (2012). If both direct and indirect radiative effects from aerosols are included in an integrated model, then an integrated model might reduce biases in surface temperature predictions to some extent without nudging. However, large biases may still exist for certain polluted sites (e.g., NYC) without nudging. This is mainly due to the inherent uncertainties in the model representations of physical and chemical processes. Polluted sites that are associated with large surface energy balance errors (e.g., NYC) may not benefit from using integrated models in terms of accurately predicting surface temperatures. However, for large domain averages (continental and semi-continental averages), model biases may be reduced if the integrated modeling systems are used.

4. Summary

Using the WRF model with FASDAS and FDDA nudging methodologies, regional climate simulations were conducted for the eastern and central U.S. for June, July, and August 2006. The results show that with prescribed aerosol optical properties included in the radiation calculation, the domain-averaged summer mean PRE_sfc, PRE_atm, and PRE_toa are −5.2, −0.8, and −6.1 W m^{-2}, respectively, whereas the domain-averaged summer mean ARE_sfc, ARE_atm, and ARE_toa are −7.4, +5.5, and −1.9 W m^{-2}, respectively. Based on model configuration used in this work, which is very popular in the WRF modeling community, in the absence of nudging the simulated climate system (based on TOA) for the entire domain may be erroneously warmed up by about 6.1 W m^{-2} while local climates (for a city or locale) can erroneously be much cooler or warmer. At all scales, errors in the surface energy balance are found to dominate high resolution regional climate modeling simulations. The domain-averaged PRE_sfc is smaller than ARE_sfc estimated in previous studies and this work, indicating FASDAS used in this work may not overwhelm aerosol radiative effects at

surface. The domain-averaged PRE_atm is much smaller than estimated ARE_atm, mainly due to significant aerosol absorption in troposphere and weak tropospheric nudging, indicating nudging may not overwhelm aerosol radiative effects in atmosphere if appropriated nudging methodology is applied to the integrated models. But PRE could be much larger than ARE at some local scales (e.g., SGP). Using an integrated modeling system might reduce radiative effects biases for large domain averages, but may not for local scales. The conclusion drawn in this work is based on the results obtained from using a specific model (i.e., WRF) with a specific model configuration. These results may differ from that obtained using other models, or if alternate physics options are used. Integrated meteorology-chemistry models can be used in the future to estimate full aerosol radiative effects and compare with PRE.

Supplementary Material

Refer to Web version on PubMed Central for supplementary material.

Acknowledgements

The research was funded by US EPA's Air, Climate, and Energy (ACE) Program (100). Our appreciation goes to Russ Bullock and Christian Hogrefe of the US EPA and Jerome Fast of the Pacific Northwest National Laboratory for their valuable comments on this work. Our appreciation also goes to Tanya Spero, Jerry Herwehe, and Chris Nolte for sharing needed data and codes used in this research. This research has been subjected to the US EPA's administrative review and approved for publication. The views expressed and the contents are solely the responsibility of the authors, and do not necessarily represent the official views of the US EPA. Part of this work is supported by the "Zhejiang 1000 Talent Plan" and Research Center for Air Pollution and Health in Zhejiang University and also by the National Natural Science Foundation of China (21577126 and 41561144004) and Department of Science and Technology of China (No. 2014BAC22B06). When this article is published, readers can access or find all data supporting our results and conclusions presented in this article at https://edg.epa.gov/.

References

Alapaty K, Niyogi D, Chen F, Pyle P, Chandrasekar A, Seaman N, 2008 Development of the flux-adjusting surface data assimilation system for meso-scale models. J. Appl. Meteor. Climatol 47, 2331–2350. 10.1175/2008JAMC1831.1.

Alapaty K, Kain JS, Herwehe JA, Bullock OR, Jr., Mallard MS, Spero TL, Nolte CG, 2014 Multiscale Kain-Fritsch Scheme: Formulations and Tests, oral presentation at 13th Annual CMAS Conference, October 27–29, 2014, Chapel Hill, NC.

Alapaty K, Glotfelty T, He J, Deng AJ, Wang W, and Herwehe J 2016 A coupled surface nudging scheme for use in retrospective weather & climate simulations for environmental applications, oral presentation at the 17th Annual WRF Users' Workshop, June 27-July 1, 2016, Boulder, CO http://www2.mmm.ucar.edu/wrf/users/workshops/WS2016/oral_presentations/5b.2.pdf.

Bellouin N, Quaas J, Morcrette J-J, Boucher O, 2013 Estimates of aerosol radiative forcing from the MACC re-analysis. Atmos. Chem. Phys 13, 2045–2062. 10.5194/acp-13-2045-2013.

Binkowski FS, Roselle SJ, 2003 Models-3 Community Multiscale Air Quality (CMAQ) model aerosol component, 1, model description. J. Geophys. Res 108, 4183 10.1029/2001JD001409.

Bowden JH, Otte TL, Nolte CG, Otte MJ, 2013 Simulating the impact of the large-scale circulation on the 2-m temperature and precipitation climatology. Clim. Dyn 40, 1903–1920. 10.1007/s00382-012-1440-y.

Bullock OR, Alapaty K, Herwehe JA, Mallard MS, Otte TL, Gilliam RC, Nolte CG, 2014 An observation-based investigation of nudging in WRF for downscaling surface climate information to 12-km grid spacing. J. Appl. Meteor. Climatol 53, 20–33. 10.1175/JAMC-D-13-030.1.

Chen F, Dudhia J, 2001 Coupling an advanced land-surface/hydrology model with the Penn State/NCAR MM5 modeling system. Part I: model description and implementation. Mon. Weather Rev 129, 569–585.

Daly C, Neilson RP, Phillips DL, 1994 A statistical-topographic model for mapping climatological precipitation over mountainous terrain. J. Appl. Meteor 33, 140–158. 10.1175/1520-0450(1994)033, 0140: ASTMFM.2.0.CO;2.

Ek MB, Mitchell KE, Lin Y, Rogers E, Grunmann P, Koren V, Gayno G, Tarpley JD, 2003 Implementation of Noah land surface model advances in the National Centers for Environmental Prediction operational mesoscale Eta model. J. Geophys. Res 108 (D22), 8851.

Fast JD, Gustafson WI, Jr., Easter RC, Zaveri RA, Barnard JC, Chapman EG, Grell GA, Peckham SE, 2006 Evolution of ozone, particulates and aerosol direct radiative forcing in the Vicinity of Houston using a fully coupled meteorology-chemistry-aerosol model. J. Geophys. Res 111, D21305 10.1029/2005JD006721.

Forkel R, Werhahn J, Hansen AB, McKeen S, Peckham S, Grell G, Suppan P, 2012 Effect of aerosol-radiation feedback on regional air quality - a case study with WRF/Chem. Atmos. Environ 53, 202–211.

Forkel R, Balzarini A, Baró R, Curci G, Jiménez-Guerrero P, Hirtl M, Honzak L, Im U, Lorenz C, Pérez JL, Pirovano G, San José R, Tuccella P, Werhahn J, Zabkar R, 2015 Analysis of the WRF-Chem contributions to AQMEII phase2 with respect to aerosol radiative feedbacks on meteorology and pollutant distribution. Atmos. Environ 115, 630–645.

Gilliam RC, Godowitch JM, Rao ST, 2012 Improving the horizontal transport in the lower troposphere with four dimensional data assimilation. Atmos. Environ 53, 186–201.

Godowitch JM, Gilliam RC, Rao ST, 2011 Diagnostic evaluation of the chemical and transport processes in a regional photochemical air quality modeling system. Atmos. Environ 45, 3977–3987.

Grell GA, Peckham SE, Schmitz R, McKeen SA, Frost G, Skamarock WC, Eder B, 2005 Fully coupled online chemistry within the WRF model. Atmos. Environ 39, 6957–6975.

He J, Zhang Y, Tilmes S, Emmons L, Lamarque J-F, Glotfelty T, Hodzic A, Vitt F, 2015 CESM/CAM5 improvement and application: comparison and evaluation of updated CB05_GE and MOZART-4 gas-phase mechanisms and associated impacts on global air quality and climate. Geosci. Model Dev 8, 3999–4025. 10.5194/gmd-8-3999-2015.

Heald CL, Ridley DA, Kroll JH, Barrett SRH, Cady-Pereira KE, Alvarado MJ, Holmes CD, 2014 Contrasting the direct radiative effect and direct radiative forcing of aerosols. Atmos. Chem. Phys 14, 5513–5527. 10.5194/acp-14-5513-2014.

Hogrefe C, Pouliot G, Wong D, Torian A, Roselle S, Pleim J, Mathur R, 2015 Annual application and evaluation of the online coupled WRF-CMAQ system over North America under AQMEII phase 2. Atmos. Environ 115, 683–694.

Hong S, Noh Y, Dudhia J, 2006 A new vertical diffusion package with an explicit treatment of entrainment processes. Mon. Weather Rev 134, 2318–2341.

Iacono MJ, Delamere JS, Mlawer EJ, Shephard MW, Clough SA, Collins WD, 2008 Radiative forcing by long-lived greenhouse gases: calculations with the AER radiative transfer models. J. Geophys. Res 113, D13103.

Jacob DJ, Winner DA, 2009 Effect of climate change on air quality. Atmos. Environ 43, 51–63.

Ji ZM, Kang SC, 2013 Double nested dynamical downscaling experiments over the Tibetan Plateau and their projection of climate change under RCPs scenarios. J. Atmos. Sci 70, 1278–1290.

Ji ZM, Kang SC, 2015 Evaluation of extreme climate events using a regional climate model for China. Int. J. Climatol 35, 888–902.

Jöckel P, Tost H, Pozzer A, Brühl C, Buchholz J, Ganzeveld L, Hoor P, Kerkweg A, Lawrence MG, Sander R, Steil B, Stiller G, Tanarhte M, Taraborrelli D, van Aardenne J, Lelieveld J, 2006 The atmospheric chemistry general circulation model ECHAM5/MESSy1: consistent simulation of ozone from the surface to the mesosphere. Atmos. Chem. Phys 6, 5067–5104.

Kassianov E, Barnard J, Pekour M, Berg LK, Michalsky J, Lantz K, Hodges G, 2013 Do diurnal aerosol changes affect daily average radiative forcing? Geophys. Res. Lett 40, 3265–3269. 10.1002/grl.50567.

Kumar R, Barth MC, Pfister GG, Naja M, Brasseur GP, 2014 WRF-Chem simulations of a typical pre-monsoon dust storm in northern India: influences on aerosol optical properties and radiation budget. Atmos. Chem. Phys 14, 2431–2446. 10.5194/acp-14-2431-2014.

Leibensperger EM, Mickley LJ, Jacob DJ, Chen W-T, Seinfeld JH, Nenes A, Adams PJ, Streets DG, Kumar N, Rind D, 2012 Climatic effects of 1950–2050 changes in US anthropogenic aerosols - Part 1: aerosol trends and radiative forcing. Atmos. Chem. Phys 12, 3333–3348. 10.5194/acp-12-3333-2012.

Lohmann U, Feichter J, 2005 Global indirect aerosol effects: a review. Atmos. Chem. Phys 5, 715–737. 10.5194/acp-5-715-2005.

Mahfouf J-F, 1991 Analysis of soil moisture from near-surface parameters: a feasibility study. J. Appl. Meteo 30, 1534–1547 doi: 10.1175/1520-0450(1991)030<1534:AOSMFN>2.0.CO;2.

Matus AV, 2013 A Global Survey of Aerosol Direct Effects. Master Thesis. University of Wisconsin-Madison August 2013.

Mlawer EJ, Taubman SJ, Brown PD, Lacono MJ, Clough SA, 1997 RRTM, a validated correlated-k model for the longwave. J. Geophys. Res 102, 16663–16682.

Monin AS, Obukhov AM, 1954 Basic laws of turbulent mixing in the surface layer of the atmosphere. Tr. Akad. Nauk. SSSR Geophiz. Inst 24 (151), 163–187.

Morrison H, Thompson G, Tatarskii V, 2009 Impact of cloud microphysics on the development of trailing stratiform precipitation in a simulated Squall line: comparison of one- and two-moment schemes. Mon. Wea. Rev 137, 991–1007. 10.1175/2008MWR2556.1.

Otte TL, Nolte CG, Otte MJ, Bowden JH, 2012 Does nudging squelch the extremes in regional climate modeling? J. Clim 25, 7046–7066. 10.1175/JCLI-D-12-00048.1.

Stauffer DR, Seaman NL, 1994 Multiscale four-dimensional data assimilation. J. Appl. Meteor 33, 416–434 doi: 10.1175/1520-0450(1994)033<0416:MFDDA>2.0.CO;2.

Stauffer DR, Seaman NL, 1990 Use of four-dimensional data assimilation in a limited-area model. Part I: experiments with synoptic-scale data. Mon. Wea. Rev 118, 1250–1277.

Tilmes S, Lamarque J-F, Emmons LK, Kinnison DE, Ma P-L, Liu X, Ghan S, Bardeen C, Arnold S, Deeter M, Vitt F, Ryerson T, Elkins JW, Moore F, Spackman R, Martin MV, 2015 Description and evaluation of tropospheric chemistry and aerosols in the community earth system model (CESM1.2). Geosci. Model Dev 8, 1395–1426. 10.5194/gmd-8-1395-2015.

Vautard R, Moran MD, Solazzo E, Gilliam RC, Matthias V, Bianconi R, Chemel C, Ferreira J, Geyer B, Hansen AB, Jericevic A, Prank M, Segers A, Silver JD, Werhahn J, Wolke R, Rao ST, Galmarini S, 2012 Evaluation of the meteorological forcing used for the air quality model evaluation international initiative (AQMEII) air quality simulations. Atmos. Environ 53, 15–37.

Wang K, Yahya K, Zhang Y, Wu S-Y, Grell G, 2015 Implementation and initial application of new chemistry-aerosol options in WRF/chem for simulating secondary organic aerosols and aerosol indirect effects for regional air quality. Atmos. Environ 115, 716–732.

Wong DC, Pleim J, Mathur R, Binkowski F, Otte T, Gilliam R, Pouliot G, Xiu A, Young JO, Kang D, 2012 WRF-CMAQ two-way coupled system with aerosol feedback: software development and preliminary results. Geosci. Model Dev 5, 299–312. 10.5194/gmd-5-299-2012.

Yu H, Kaufman YJ, Chin M, Feingold G, Remer LA, Anderson TL, Balkanski Y, Bellouin N, Boucher O, Christopher S, DeCola P, Kahn R, Koch D, Loeb N, Reddy MS, Schulz M, Takemura T, Zhou M, 2006 A review of measurement-based assessments of the aerosol direct radiative effect and forcing. Atmos. Chem. Phys 6, 613–666. 10.5194/acp-6-613-2006.

Yu S, Mathur R, Pleim J, Wong D, Gilliam R, Alapaty K, Zhao C, Liu X, 2014 Aerosol indirect effect on the grid-scale clouds in the two-way coupled WRFCMAQ: model description, development, evaluation and regional analysis. Atmos. Chem. Phys 14, 11247–11285. 10.5194/acp-14-11247-2014.

Zhang Y, 2008 Online coupled meteorology and chemistry models: history, current status, and outlook. Atmos. Chem. Phys 8, 2895–2932.

Zhang K, Wan H, Liu X, Ghan SJ, Kooperman GJ, Ma P-L, Rasch PJ, Neubauer D, Lohmann U, 2014 Technical Note: on the use of nudging for aerosol-climate model intercomparison studies. Atmos. Chem. Phys 14, 8631–8645. 10.5194/acp-14-8631-2014.

Zheng Y, Alapaty K, Herwehe J, Del Genio A, Niyogi D, 2016 Improving high-resolution weather forecasts using the Weather Research and Forecasting (WRF) model with an updated Kain-Fritsch scheme. Mon. Wea. Rev 144, 833–860. 10.1175/MWR-D-15-0005.1.

Highlights

- Temperature changes due to nudging are converted to pseudo radiative effects (PRE).
- The domain mean PRE is smaller than aerosol effects at surface and in atmosphere.
- Nudging could be applied to the integrated models to study ARE at regional scales.
- Integrated models with nudging need be treated with caution to study local scale ARE.

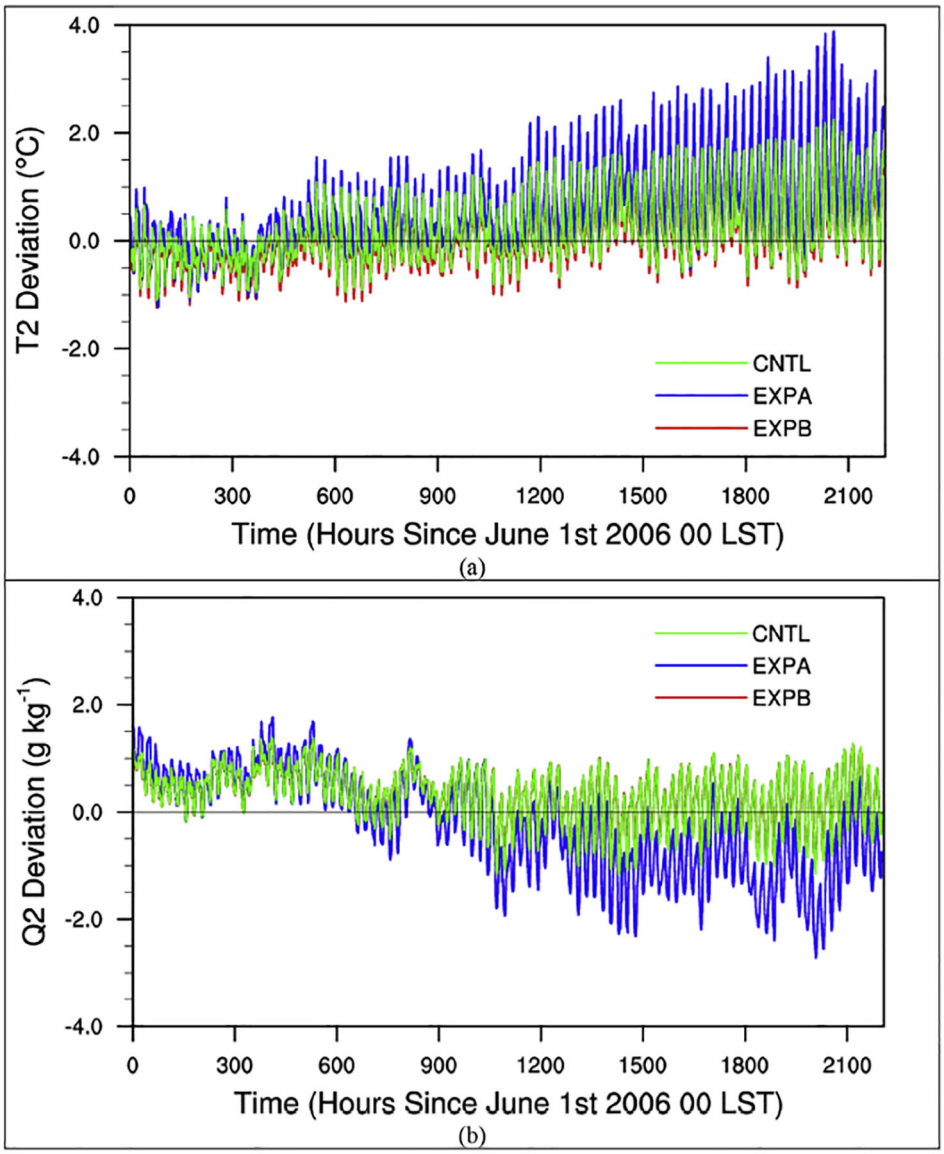

Fig. 1.

Time series of 2-m temperature (T2) and 2-m water vapor mixing ratio (Q2) deviations (i.e., sim – obs) from Quality Controlled Local Climatological Data based on model simulations.

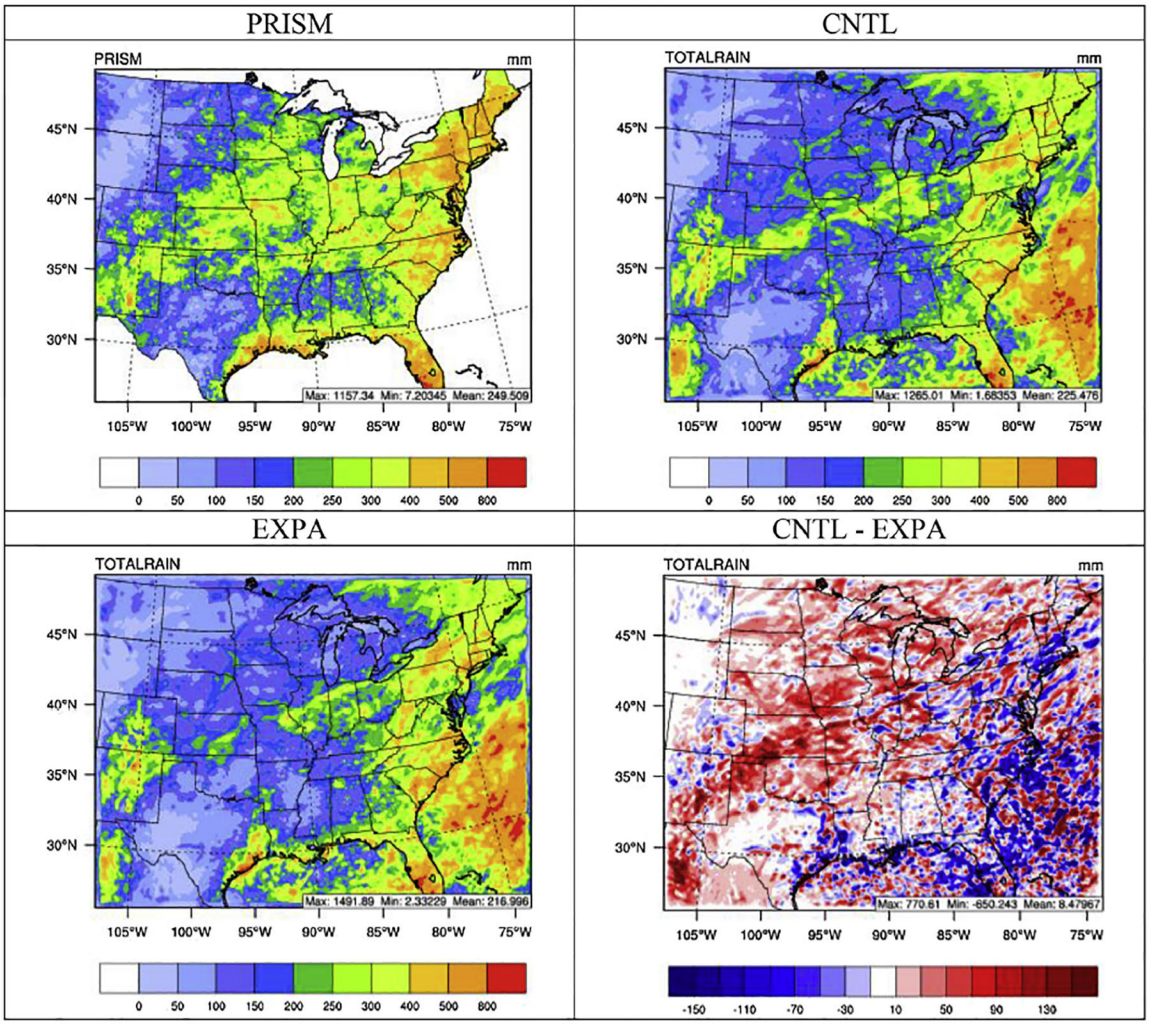

Fig. 2.

Comparison of accumulated precipitation of June-July-August 2006.

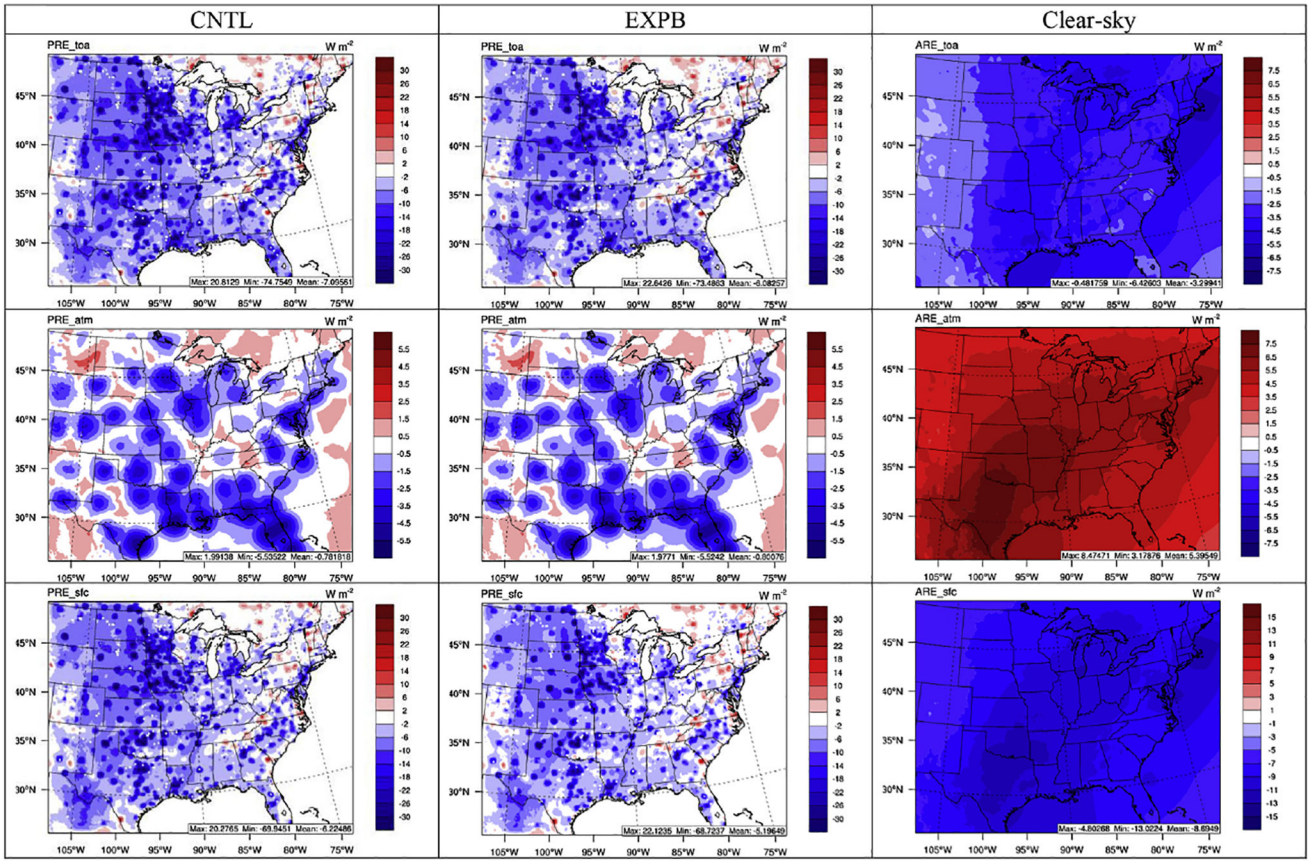

Fig. 3.

The spatial distribution of June-July-August (JJA) averaged PRE in CNTL (left column) and EXPB (middle column), at the surface (PRE_sfc), in atmosphere (PRE_atm), and at the top of atmosphere (PRE_toa), and clear-sky ARE (right column) at the surface (ARE_sfc), in atmosphere (ARE_atm), and at the top of atmosphere (ARE_toa).

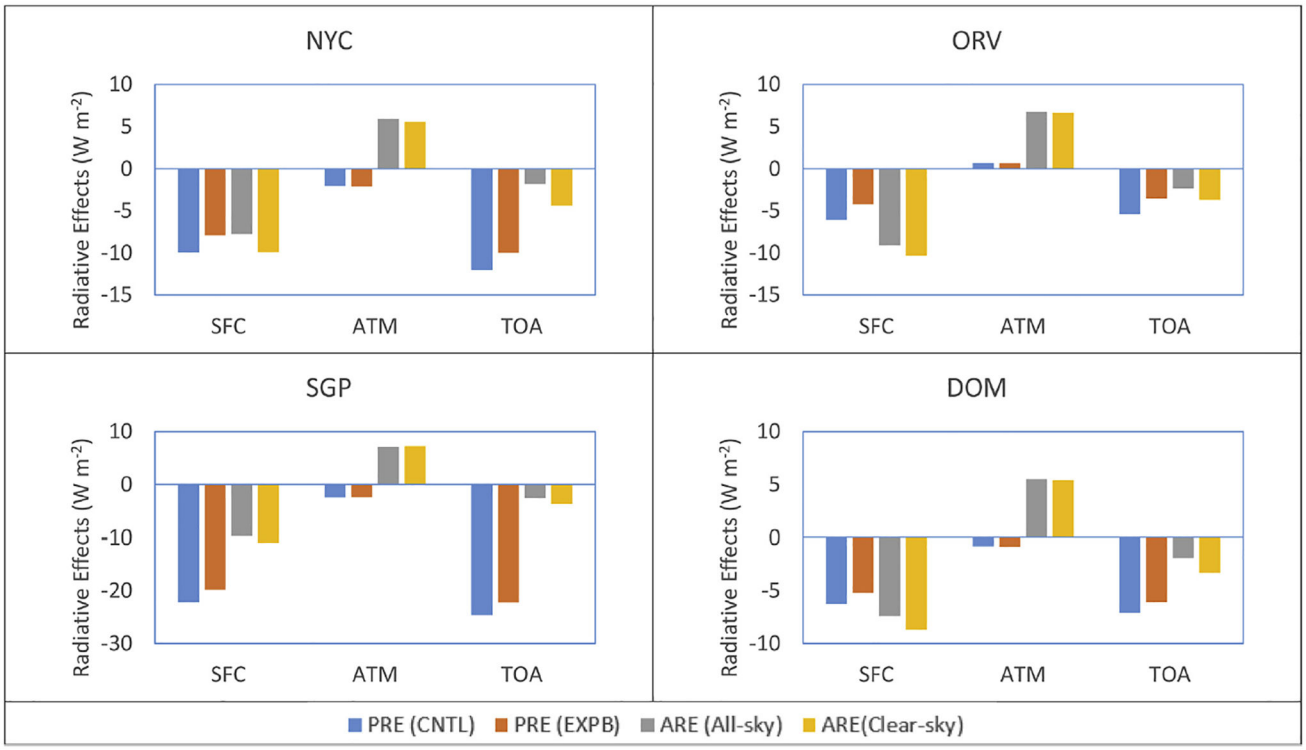

Fig. 4.

June-July-August (JJA) mean PRE and clear-sky ARE at the surface (PRE_sfc and ARE_sfc), in atmosphere (PRE_atm and ARE_atm) and at the top of atmosphere (PRE_toa and ARE_toa) for the New York City site (NYC), the Ohio River Valley site (ORV), the Southern Great Plains site (SGP), and the domain-wide average (DOM), respectively.

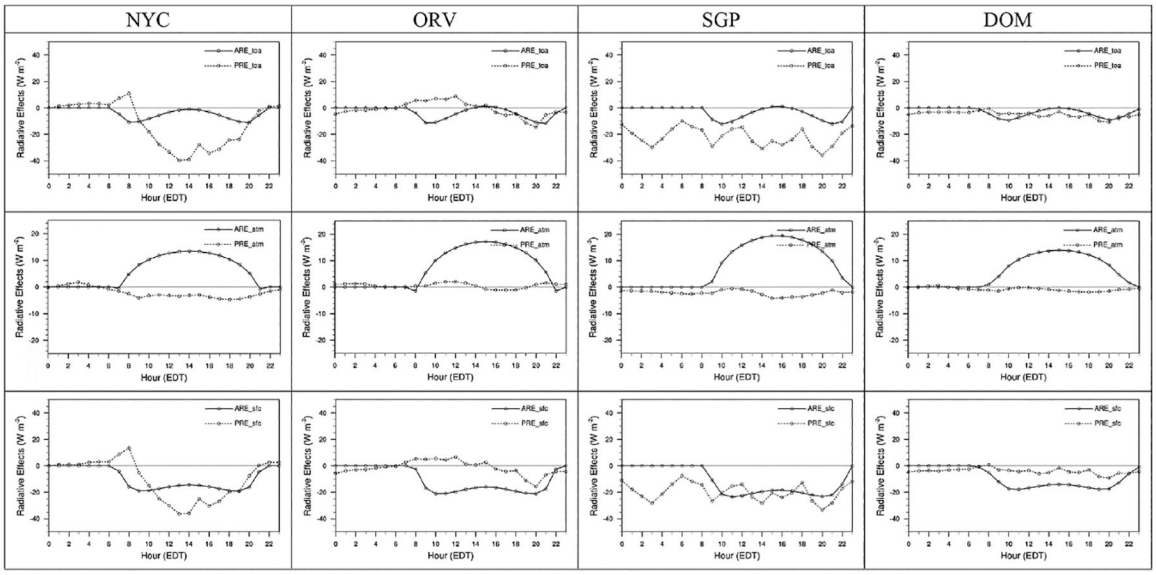

Fig. 5.

Diurnal variation for PRE and ARE at the top of atmosphere (PRE_toa and ARE_toa, row 1), in atmosphere (PRE_atm and ARE_atm, row 2), and at the surface (PRE_sfc and ARE_sfc, row 3) for the New York City site (NYC), the Ohio River Valley site (ORV), the Southern Great Plains site (SGP), and the domain-wide average (DOM), respectively.

Table 1

Simulation design and purpose.

Simulation Index	Configuration	Purposes
CNTL	Continuous simulation with FDDA for free troposphere and FASDAS for surface; aerosols are excluded in the radiation calculation (i.e., aer_opt = 0)	Serves as baseline
EXPA	Same as CNTL, but with FDDA for free troposphere only	The differences between CNTL and EXPA indicate the impacts of FASDAS on model predictions.
EXPB	Same as CNTL, but with double calling method in radiation scheme to estimate differences in shortwave fluxes between prescribed aerosol condition (i.e., aer_opt = 1) and no aerosol condition (i.e., aer_opt = 0).	To estimate aerosol radiative effects

Table 2

Reported aerosol direct/indirect radiative effects (DRE/IRE).

	CONUS	Global	References
Top of atmosphere		~ −0.5 to −5 (IRE, land, all-sky)	Lohmann and Feichter (2005)
	< −10 (DRE, clear-sky)	−6.4 ± 1.0 (DRE, land, clear-sky)	Bellouin et al. (2013)
	−5.2 to −11.1 (AERONET DRE, clear-sky)	−4.9 ± 0.7 (DRE, land, clear-sky)	Yu et al. (2006)
	−4.0 to −8.7 (satellite, DRE, clear-sky)		
	~ −4 (DRE, clear-sky)		Heald et al. (2014)
	~ −2 (DRE, all-sky)		
	~ −2.5 (obs. DRE, all-sky)		Matus (2013)
	~ −3 (model DRE, all-sky)		
	−1.9 (DRE, all-sky)		This work
	−3.3 (DRE, clear-sky)		
Atmosphere		+ 5.1 (DRE, land, clear-sky)	Bellouin et al. (2013)
	~ +13.0 (obs. DRE, all-sky)		Matus (2013)
	~ +4.5 (model DRE, all-sky)		
	+ 5.5 (DRE, all-sky)		This work
	+ 5.4 (DRE, clear-sky)		
Surface		−11.5 ± 1.9 (DRE, land, clear-sky)	Bellouin et al. (2013)
	−14.4 to −23.9 (AERONET[a], DRE, clear-sky)	−11.8 ± 1.9 (DRE, land, clear-sky)	Yu et al. (2006)
	−16.2 (overall effects, all-sky)		Wang et al. (2015)
	−4.1 (DRE, all-sky)		
	−12.1 (IRE, all-sky)		
	~ −15.0 (obs. DRE, all-sky)		Matus (2013)
	~ −7.0 (model DRE, all-sky)		
	−7.4 (DRE, all-sky)		This work
	−8.7 (DRE, clear-sky)		

[a]AERONET: the AEROsol Robotic Network.